



Advances in Research

17(1): 1-20, 2018; Article no.AIR.44062
ISSN: 2348-0394, NLM ID: 101666096

A New Dynamical Theory of Decompression

Pierre Boudinet^{1,2*}

¹Lycée Raoul Follereau, Belfort, France.

²Fédération Française de Spéléologie (French Federation of Speleology), France.

Author's contribution

The sole author designed, analysed, interpreted and prepared the manuscript.

Article Information

DOI: 10.9734/AIR/2018/44062

Editor(s):

(1) Dr. Oswin Grollmuss, Professor, Department of Pediatric and Adult Resuscitation, Congenital Heart of Centre Chirurgical Marie Lannelongue, University Paris XI, France.

(2) Dr. Martin Kröger, Professor, Computational Polymer Physics, Swiss Federal Institute of Technology (ETH Zürich), Switzerland.

(3) Dr. Jinyong Peng, Professor, College of Pharmacy, Dalian Medical University, Dalian, China.

Reviewers:

(1) Yahaya Shagaiya Daniel, Kaduna State University, Nigeria.

(2) Bruce Wienke, USA.

(3) Li Wei, Research Center of Fluid Machinery Engineering and Technology, Jiangsu University, China.

Complete Peer review History: <http://www.sciencedomain.org/review-history/27021>

Received 22 August 2018

Accepted 29 October 2018

Published 03 November 2018

Original Research Article

ABSTRACT

We present a new way of taking in account the dynamics of the gas phase during decompression. This preliminary study, although being potentially capable of dealing with extreme dives, far from the no-stop limit, is not developed as a practical tool yet. It is based on the analysis of certain hypotheses underlying classical models using Maximal Values (M-Values). We derive a reduced set of ordinary differential equations, depending only on three empirical parameters. After having explained how the theory is built, we propose some values of the parameters that match the known surface M-Values well. Then we examine, for a single compartment, the theoretical predictions in the case of an abnormal situation (missing decompression stops) and in the case of dives with mixes containing helium (trimix and heliox). The results are more realistic than those of neo-Haldanian models. This new theory is capable of explaining why decompression accidents cannot occur immediately and why they can be delayed. The efficiency of oxygen breathing in such a situation is also well explained. More generally, the tolerance to inert gases depends on the breathed mix. In the present state, this theory, which is different from the Reduced Gradient Bubble Model (RGBM) and Variable Permeability Model (VPM), has an explanatory power that goes beyond the simple computation of decompression stops. Once developed as a full model, validated and definitively tuned, it could lead to a probabilistic approach of the safety, which is required by the extreme dives performed when exploring certain syphons.

*Corresponding author: E-mail: pierre.boudinet@ac-besancon.fr, p.boudinet@free.fr;

Keywords: Diving; decompression; Neo-Haldanian; theory; syphon; risk level; M-values.

1. INTRODUCTION

The most used decompression models, through tables, softwares or diving computers, are based on Neo-Haldanian theories [1], deriving from Haldane's original work [2]. Because they are based upon unsupported assumptions, alternative models using more physical principles have been developed. The Variable Permeability Model (VPM) [3], as well as the Reduced Gradient Bubble Model (RGBM) [4], take into account the dynamics of the gas phase. As neo-Haldanian models do not so, they can apply only to the simple enough situations from which they have been tuned, mostly dives that do not include too many decompression stops and that have simple profiles [5]. They cannot be regarded as reliable for intricate dives, for instance those encountered during cave diving where several syphons of variable depth have to be passed, often in remote places and far from any recompression chamber. However, VPM and RGBM themselves rely on particular assumptions that could be discussed: In VPM, bubbles are supposed to be spherical. Well-known in-vitro models of bubble nucleation are extrapolated to in-vivo situations [3,4,6]. Many models establish a duality between "safe" or "unsafe" desaturation situations, whereas the occurrence of decompression sickness is a probabilistic phenomenon as evoked for example in [7].

This is why we developed an alternative theory, also capable of taking in account the dynamics of the gas phase (bubbles) in normal or abnormal situations. On the contrary of RGBM and VPM, we put the emphasis on dimensional analysis and dimensional reduction rather than on very detailed physical processes. The result is a theory that depends only upon three parameters, that have to be adjusted to match already known data. This small number of parameters, their generality and simplicity, make the uniqueness of the study. It derives from the analysis of internal correlations and discrepancies inherent to several neo-Haldanian models [4,8]. This includes Workman's studies (USA) [9], the models of Bühlmann (Switzerland) [10] such as ZHL-16, and the model corresponding to the French military tables (MN90) [11]. The French commercial tables (MT92) are probably close to Haldanian models, although taking in account more precisely the influence of circulating bubbles [12]. Unfortunately, precise data and

complete calculations are not available. Therefore the MT92 are not included in the present study.

Neo-Haldanian models implicitly take into account the formation of gas phase during the decompression. At a given ambient pressure (given depth), if the tension (partial pressure) of inert gas dissolved during the dive in a given compartment is too important and exceeds a maximal value ("M-Value" [13]), then it is assumed that pathological bubbles form. Our theory keeps this idea but does neither assume that bubbles form instantaneously nor that the existence of bubbles has no influence upon the desaturation process. The fact that the largest M-Values correspond to the quickest compartments must draw attention. Explaining this fact is one of the key features of our work and contributes to its uniqueness. We translate quantitatively the following qualitative reasoning: the shorter the period of a compartment is, the faster the tension of inert gases will decrease; the quicker the tensions of inert gases decrease, the more difficult it is for bubbles to grow inside the compartment. If bubbles large enough trigger decompression sickness, then the relevant parameter is the critical extension of the gas phase (size of the bubbles): The empirical knowledge of all the M-Values is superseded by the knowledge of two parameters characterising critical bubbles: their size and their characteristic formation time (corresponding to an "inner halftime").

The M-Values of different neo-Haldanian models varies in an affine way according to the depth. This can be explained by the fact that the pressure inside the gas phase is different, slightly higher than the external pressure (ambient pressure). However, this pressure gradient varies from compartment to compartment, and from model to model. The M-Values for helium differ from their counterpart for nitrogen: as helium is less soluble than nitrogen and diffuses more quickly, there should be particular relationships between both M-Values. Again, there are differences from model to model, and from compartment to compartment. These two discrepancies suggest that this kind of static modelling is not sufficient: the pressure gradient of the gas phase and the specificities of helium transportation must be more completely taken into account. This is another key feature of our work. We take into account the pressure

gradient as a third parameter and consider all the possibilities regarding helium transportation (diffusion, perfusion, intermediate situations).

2. MATERIALS AND METHODS

2.1 Quantitative Analysis of Different Neo-Haldanian Models – Pressure Gradient and Critical Volume

Whatever their precise location and shape, if bubbles appear in a compartment their inner pressure isn't strictly equal to the ambient pressure P_{amb} . Taking in accounts the effects of the superficial tension, the value of the inner pressure is $P_{amb} + \delta P$.

If P_{N_2} , P_{He} stand for the tensions of nitrogen and helium in a given compartment of volume V_{comp} , if α_{N_2} , α_{He} stands for the solubilities of nitrogen and helium (mol per unit of volume and bar), the quantities of matter (mol) in that compartment, according to Henry's law, are:

$$N_{N_2} = \alpha_{N_2} P_{N_2} V_{comp} \quad (1)$$

$$N_{He} = \alpha_{He} P_{He} V_{comp} \quad (2)$$

If the ambient pressure decreases suddenly, the quantities of matter are conserved and neo-Haldanian models assume that bubbles of total volume V_b , whose content is in equilibrium with the rest of the compartment, form immediately. Neglecting the water and carbon dioxide tensions, we obtain:

$$\alpha_{N_2} P_{N_2} V_{comp} = \eta (P_{amb} + \delta P) (\alpha_{N_2} V_{comp} + V_b / RT) \quad (3)$$

$$\alpha_{He} P_{He} V_{comp} = (1 - \eta) (P_{amb} + \delta P) (\alpha_{He} V_{comp} + V_b / RT) \quad (4)$$

η is the molar fraction of nitrogen in the bubbles, T the temperature and R the ideal gas constant.

In the case of absence of helium (diving with air or nitrogen-oxygen mixes called 'nitrox') where $\eta = 1.0$, this leads to a very simple relationship:

$$P_{N_2} = (P_{amb} + \delta P) (1 + V_b / (RT \alpha_{N_2} V_{comp}))$$

If the border between 'decompression problems' and 'no decompression problems' corresponds to a certain critical volume $V_b = V_c$ of the gas phase, then the maximal value of P_{N_2} is:

$$(P_{amb} + \delta P) (1 + V_c / (RT \alpha_{N_2} V_{comp})) \quad (5)$$

This corresponds exactly to affine relationship initially proposed by Workman and reinvestigated by other authors including Bühlmann.

The notations used by Bühlmann and Workman are slightly different and can be confusing [13]. If M_0 stands for the value of M when $P_{amb} =$ 'Atmospheric pressure at the sea level' = 1 atm = P_0 , then the current value M can be written:

$$M(P_{amb}) = M_0(P_{amb} + \delta P) / (P_0 + \delta P) = M_0 + M_0(P_{amb} - P_0) / (P_0 + \delta P)$$

$$M(P_{amb}) = M_0 + M_0(P_{amb} - P_0) / (P_0 + \delta P) = M_0 + M_0 / (P_0 + \delta P) \times \text{'relative pressure'}$$

$$M(P_{amb}) = M_0 + \Delta M \times \text{'relative pressure'}$$

Knowing the way M varies with the relative pressure (linked to the depth) enables the access to δP by:

$$+ \delta P = M_0 / \Delta M - P_0 \quad (6)$$

Fig. 1 shows that different models propose surface M -Values (M_0) that are almost identical. This is not surprising, even if the populations (civilian or military) and the dives (recreational, military or commercial) are slightly different, the criteria for safely coming back to the surface should be close. The results of Fig. 2 are more surprising, for the associated δP (computed with Eq. 6) are very different. This means that the criteria for safely coming back to a given decompression stop below the surface strongly differ according to the model. Also, as each compartment doesn't correspond to a precise part, a precise organ, of the human body, one would expect a uniform value of δP within each model, which is not the case. The values proposed by Bühlmann (according to a mathematical formula) continuously decrease as the half-time of the compartment increases, whereas the values proposed by Workman decrease and then increase. Both models propose higher pressure gradients for the faster compartments and lower δP for the slower compartments. This is perhaps because the most disabling decompression accidents (type II) are linked to compartments having a rather short half-time: regarding decompression engineering, with a given value of M_0 , the lower δP is, the slower the M -Value increases with the depth and the safer the decompression is. Whatsoever, this reveals a certain degree of incertitude. Keeping in mind that $\delta P = 0$ for the MN90, it appears that the pressure gradient is not a very well understood quantity.

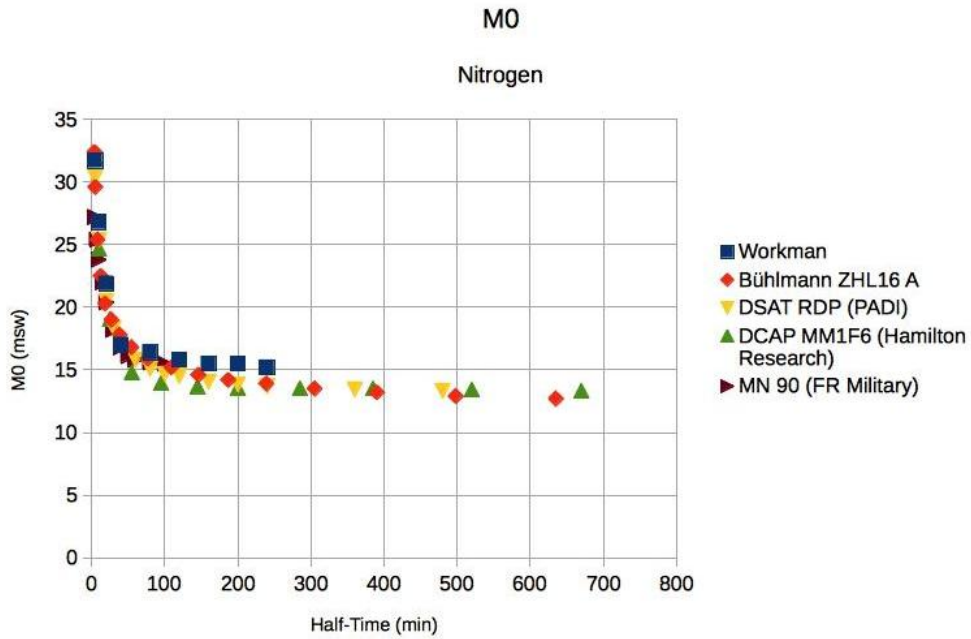


Fig. 1. Nitrogen M-Values of several models
 Pressure unit: meter of sea-water (msw)

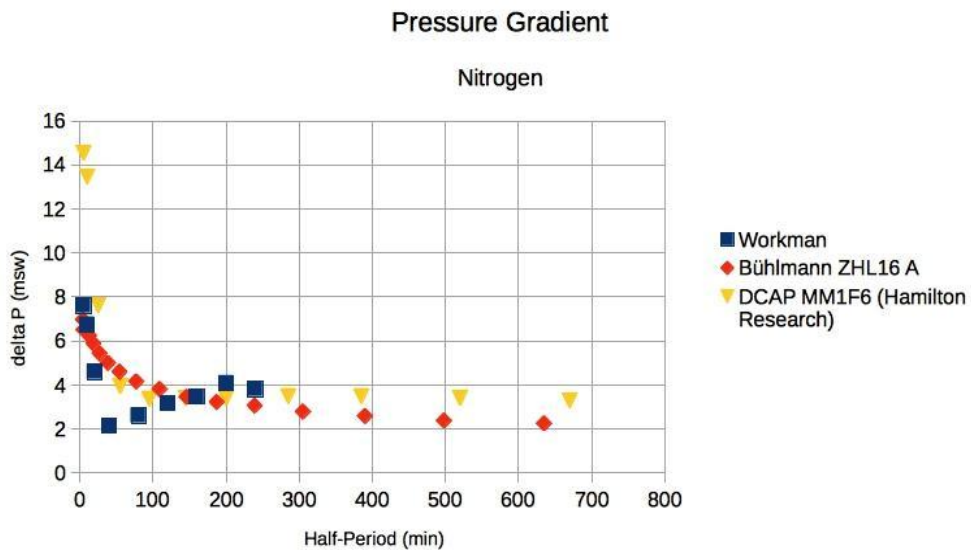


Fig. 2. Nitrogen pressure gradient of several models
 Pressure unit: meter of sea-water (msw)

In the case of helium (diving with a helium-oxygen mix: heliox), the same analysis leads to different maximal values of P_{He} :

$$(P_{amb} + \delta P)(1 + V_c / (RT\alpha_{He}V_{comp})) \quad (7)$$

If $M0'$ stands for the value of when $P_{amb} =$ 'Atmospheric pressure at the sea level' = 1 atm = P_0 then the current value M' can be re-written:

$$M'(P_{amb}) = M0'(P_{amb} + \delta P) / (P_0 + \delta P) = M(P_{amb}) = M0 + \Delta M \times \text{'relative pressure'} \quad (8)$$

The pressure gradient is now:

$$+\delta P = M0'/\Delta M' - P_0 \tag{9}$$

Not all the models deal with helium, but Fig. 3 shows that there is few difference between the $M0'$ values proposed by Workman and those proposed by Bühlmann. Again, this is not surprising, even with populations and dives slightly different, the criteria for safely coming back to the surface should be close. More

surprisingly, and in the same way of Fig. 2, Fig. 4 shows a more important dispersion of δP . Fig. 5 show the total incoherence of this quantity. At least within the frame of a given model one should expect the same value of δP for a given compartment regardless of the nature of the gas. Helium, as well as nitrogen, have no particular surface properties; on the contrary of $M0$ or $M0'$, linked to the solubilities, δP is only a mechanical quantity.

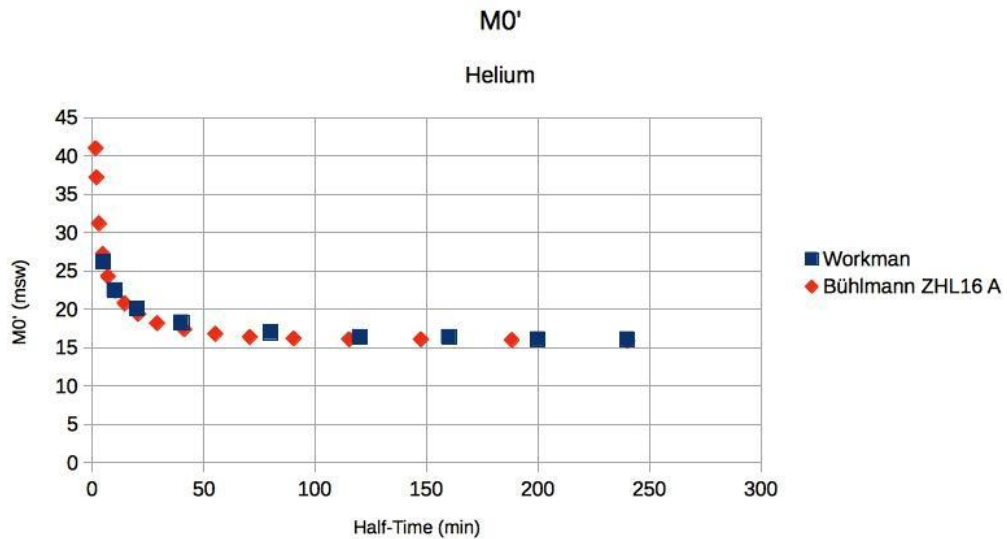


Fig. 3. Helium M-Values of two models
 Pressure unit: meter of sea-water (msw)

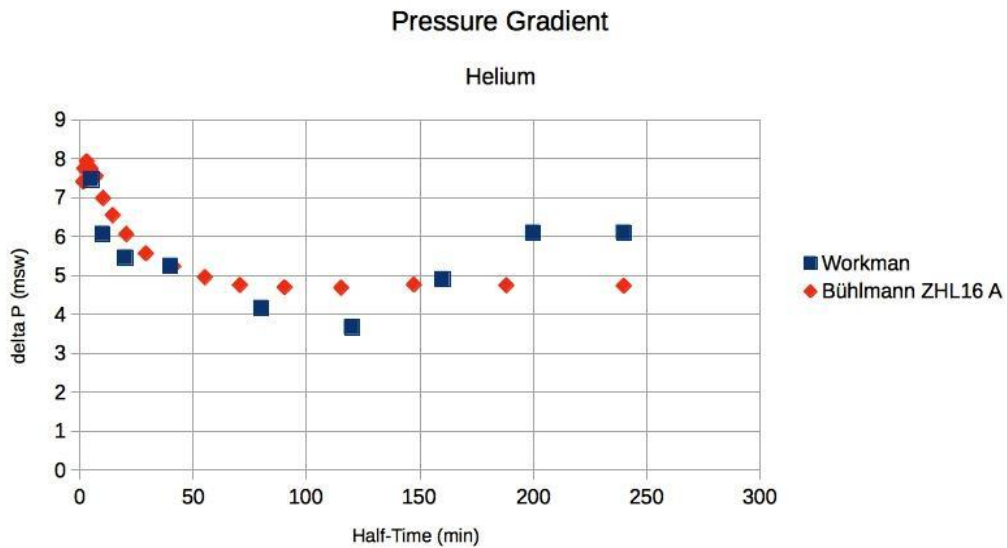


Fig. 4. Helium pressure gradient of two models
 Pressure unit: meter of sea-water (msw)

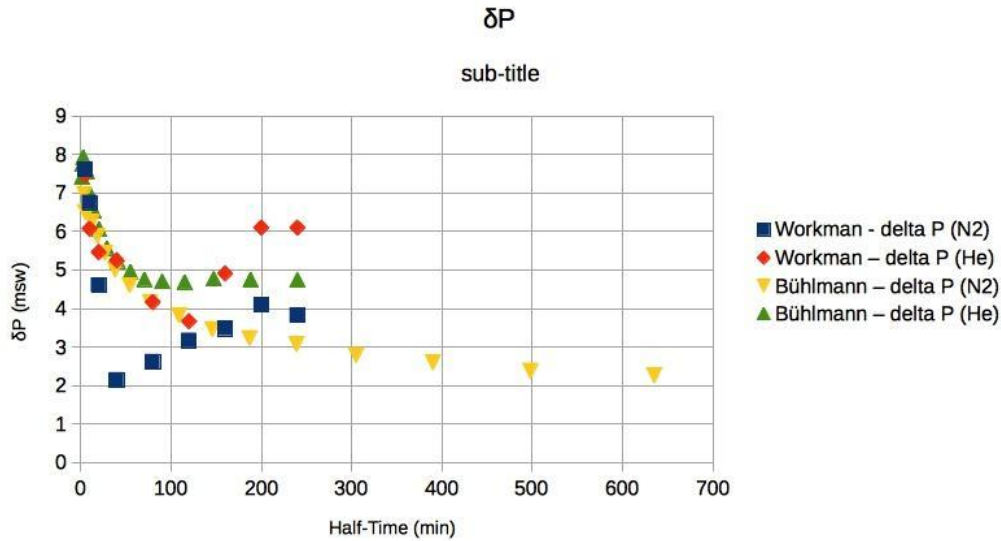


Fig. 5. Discrepancy regarding the pressure gradient
 Pressure unit: meter of sea-water (msw)

2.2 The Case of Mixes of Helium and Nitrogen – Solubilities

During a dive with a mix containing helium and nitrogen (trimix), Eq. 3 and Eq. 4 lead to the following safety criterion:

$$P_{N_2} / M_{N_2} + P_{He} / M_{He} \leq 1.0$$

M_{N_2} corresponds to Eq. 5 and M_{He} to Eq. 7

This very simple criterion is not the one retained in Bühlmann's modelling [13]: The sum of the tensions (partial pressures) of helium and nitrogen is compared to an averaged M-value. As the solubilities of helium and nitrogen are different, this kind of calculation has no physical basis. In addition, the comparison between Eq. 5 and Eq. 7 should lead to:

$$\left(\frac{M_{N_2}}{(P_{amb} + \delta P) - 1} \right) / \left(\frac{M_{He}}{(P_{amb} + \delta P) - 1} \right) = \alpha_{He} / \alpha_{N_2} \quad (10)$$

One could expect that has $\alpha_{He} / \alpha_{N_2}$ a constant value, because of the reasons above used to discuss Fig. 2. At 20°C, 1 l of water can dissolve 0.0089 l of helium or 0.016 l of nitrogen [14]. Even if the ratio slightly changes according to the temperature, and if the human body is not pure water, the quantity $\alpha_{He} / \alpha_{N_2}$ should be close to 0.56.

However, Fig. 6 shows very different values. The values proposed by Workman are more

dispersed, but even the values proposed by Bühlmann are not constant and can differ from 0.56.

One can point out the fact that Workman modeling assumes compartments limited only by perfusion (the helium period is the same as the nitrogen period) whereas Bühlmann modeling assumes compartments limited only by diffusion (the helium period is shorter than the nitrogen period, with a ratio close to 2.64. Fig. 6 represents $\alpha_{He} / \alpha_{N_2}$ versus helium halftime.

2.3 Design of a Dynamical Theory

2.3.1 Specifications and concept

All the discrepancies revealed above have led us to build a theory that:

First, is compatible with the known values of gives values of $M0$ and $M0'$;

Second, uses the lowest possible number of empirical parameters uses physical quantities (such as a critical volume) common to all the compartments;

Third, is coherent with the known variations of the M-Values according to depth;

Fourth, takes into account the fact a compartment is not limited only by the diffusion or only by the perfusion. A compartment having a

given period for nitrogen (most common diluent gas) corresponds in fact to several compartments having different periods for helium. The assumptions made by Workman or Bühlmann are only limited cases as pointed out above.

We take into account the formation of gas phase inside each compartment once the tensions of inert gases are important enough, during desaturation. The compartment saturates according to exponential laws like neo-Haldanian models (Fig. 7A). However, the gas phase, when it exists, changes the boundary conditions regarding the transportation inside a given compartment (mainly by diffusion, Fig. 7B & Fig. 7C). This why the desaturation process is no longer symmetrical of the saturation process. As long as some gas phase exists inside a compartment, the dissolved inert gases will partly move outside the compartment and partly move towards this inner gas phase: that phase of desaturation takes place at a slower pace than saturation.

This is a dynamical process. As the quantity of inert gas dissolved inside a compartment decreases during the desaturation, the difference of tensions between the dissolved inert gases and the content of the inner gas phase will be first positive (the volume of the gas phase grows) than negative (the volume of the gas phase diminishes, then vanishes). All other quantities being fixed, the maximal extension of the inner

gas phase increases with the halftime. This is why the tolerance to inert gases is expected to decrease with the halftime, like Fig. 1 and Fig. 3. Without taking into account a strictly positive pressure gradient, the gas phase would grow as soon as the tension of inert gas equals the ambient pressure, which is not totally realistic.

2.3.2 Equations

Without gas phase, we propose the same dynamics than any other Haldanian model:

$$d(\alpha_{N_2} P_{N_2} V_{comp})/dt = K_{N_2}(X_{N_2}P_{amb} - P_{N_2}) \quad (11)$$

$$d(\alpha_{He} P_{He} V_{comp})/dt = K_{He}(X_{He}P_{amb} - P_{he}) \quad (12)$$

K_{N_2} and K_{He} are the kinetic constants of the first order law expressing the exchange of inert gases, regardless of the precise mechanism (perfusion or diffusion). X_{N_2} and X_{He} are the fractions of inert gases in the breathed mix.

With gas phase, we propose to take in account the exchange of inert gases between the compartment itself and its inner gas phase as follows:

$$d(\alpha_{N_2} P_{N_2} V_{comp})/dt = K_{N_2}(X_{N_2}P_{amb} - P_{N_2}) + K'(\eta (P_{amb} + \delta P) - P_{N_2}) \quad (13)$$

$$d(\alpha_{He} P_{He} V_{comp})/dt = K_{He}(X_{He}P_{amb} - P_{he}) + K''((1-\eta) (P_{amb} + \delta P) - P_{He}) \quad (14)$$

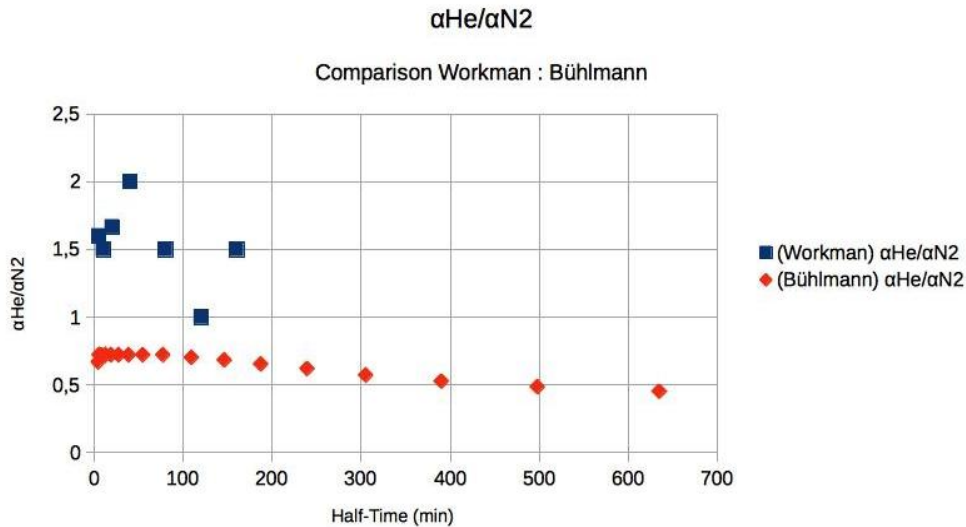


Fig. 6. Discrepancy regarding helium solubility

Abscissa: nitrogen halftime. Using the helium halftime would let Workman values untouched and shrink the abscissa of Bühlmann values

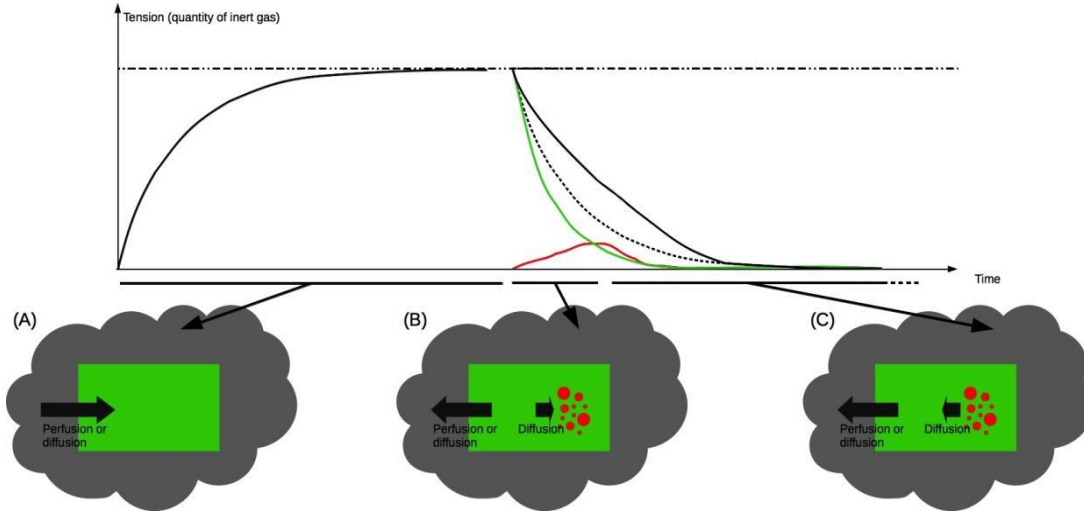


Fig. 7. Taking into account the gas phase during desaturation
Green line: quantity of inert gas dissolved inside the compartment during desaturation

Redline: extension of the gas phase

Dark line: the total quantity of inert gas inside the compartment during desaturation

Dashed line: comparison with an exponential law

A: saturation without gas phase. B: desaturation with growing gas phase. C: desaturation with decreasing gas phase

K' and K'' are the kinetic constants traducing the exchanges of nitrogen and helium between the gas phase and the rest of the compartment by diffusion. It is expected that $K'' \approx \sqrt{28}/\sqrt{4}K' \approx 2.65 K'$ because the diffusion coefficients vary approximately [15] according to the inverse of the square root of the molecular mass (Graham's law).

During this diffusion process, the matter that appears in the gas phase comes from the rest of the compartment. Therefore two other following equations appear as conservation laws:

$$d(\eta V_b (P_{amb} + \delta P)/RT)/dt = -K'(\eta (P_{amb} + \delta P) - P_{N_2}) \quad (15)$$

$$d((1-\eta) V_b (P_{amb} + \delta P)/RT)/dt = -K''((1-\eta) (P_{amb} + \delta P) - P_{He}) \quad (16)$$

Eq. 11 to 16 seem very intricate. They depend upon a large number of parameters. Indeed, they can easily simplify as explained below. When there is no gas phase, they can be rewritten as:

$$d(P_{N_2})/dt = (1/T_{N_2})(X_{N_2}P_{amb} - P_{N_2}) \quad (17)$$

$$d(P_{He})/dt = (1/T_{He})(X_{He}P_{amb} - P_{He}) \quad (18)$$

T_{N_2} and T_{He} are directly linked to the halftimes. When the gas phase exists:

$$d(P_{N_2})/dt = (1/T_{N_2})(X_{N_2}P_{amb} - P_{N_2}) + (1/\tau')(\eta (P_{amb} + \delta P) - P_{N_2}) \quad (19)$$

$$d(P_{He})/dt = (1/T_{He})(X_{He}P_{amb} - P_{He}) + (1/\tau'')((1-\eta) (P_{amb} + \delta P) - P_{He}) \quad (20)$$

The new quantity τ' , having also the dimension of a halftime, corresponds to the internal exchanges between the gas phase and the rest of the compartment. $\tau'' = \tau'/2.65 = \tau'\sqrt{4}/\sqrt{28}$ is not a new independent quantity. Introducing the dimensionless quantities $u = V_b/(\alpha_{N_2} RT V_{comp})$ and $r = \alpha_{N_2}/\alpha_{He}$, the extension of the gas phase is governed by:

$$d(u\eta(P_{amb} + \delta P))/dt = - (1/\tau')(\eta (P_{amb} + \delta P) - P_{N_2}) \quad (21)$$

$$d(ru(1-\eta)(P_{amb} + \delta P))/dt = - (1/\tau'')(\eta (P_{amb} + \delta P) - P_{He}) \quad (22)$$

The only additional parameter is δP , r being derived from tabulated values.

2.4 Computing Aspects: Building of a Library (C Language)

We have developed a library based on the C language. It can be used to develop programs regardless of the precise operating system and

processor (Windows or Unix based, computer or micro-controller, etc.) Although it is not the aim of the present article, “decompression softwares” could be built using our library, with the important reserve that the corresponding theory is not regarded as validated yet. This library is available at <https://nvdecompression.sourceforge.io> or can be asked directly to the author.

3. RESULTS AND DISCUSSION

3.1 Explanatory Power – the Case of Nitrogen

In the absence of helium, Table 1 shows that our theory can be tuned to be in good adequacy with already existing tabulated M values. We simulated the decompression of the compartments with different values of δP and τ' and we retained the more adequate maximal value of u (u_c corresponding to the critical volume V_c). A direct result of Eq. 17 to 22 is that, all other parameters being constant, the more important δP is, the more important the predicted M_0 are. The less important τ' is, the more important the predicted M_0 values of the shorter compartments are.

$\delta P = 0.2$ bar and τ' corresponding to a halftime of 20' are adequate values, along with $u_c = 0.17$. The value of δP is in-between the case of the MN90 ($\delta P = 0$) and the case of the other tables that have been presented above.

With this choice of δP and τ' , Fig. 8 compares the predicted M_0 and the tabulated values of Workman. The slight discrepancy of the quickest compartments could be explained by the fact that the model of Workman is older, based upon fewer experimental observations. It may also be explained by the fact that, during an ascent at a finite speed, the quicker compartments will evolve, more than the slower. Fig. 9 compares the predicted M_0 and the more recent tabulated values underlying the MN90 tables. It shows very good adequacy.

3.2 Explanation of Some Delayed Effects

Through Eq. 21 and Eq. 22, our theory predicts that the gas phase does not appear immediately inside a compartment at the beginning of the decompressions and that it remains for more or less time. Fig. 10 shows how the extension of the gas phase evolves when compartments, initially saturated in nitrogen with a tension corresponding to M_0 , are brought back to the surface. Even for the quickest compartments, some gas remains for more than half an hour. The gas phase in the slowest compartments can remain several hours. All that is in good adequacy with practical rules such as “not doing efforts after a dive” and gives a quantitative justification to the well-known fact that desaturation is not symmetrical from saturation [16].

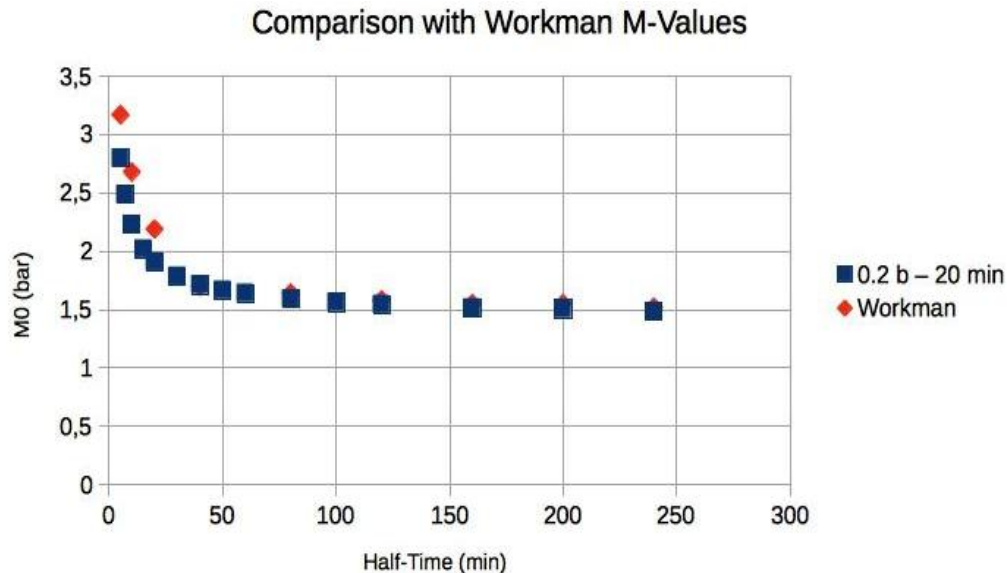


Fig. 8. Comparison of the best-predicted M-Values with those used by Workman

Table 1. Theoretical predictions of M-values

T (min)	20.0 min 0.2 b	20.0 min 0.3 b	20.0 min 0.1 b	17.5 min 0.2 b	17.5 min 0.3 b	17.5 min 0.1 b	22.5 min 0.2 b	22.5 min 0.3 b
	$u_c=0.17$	$u_c=0.12$	$u_c=0.22$	$u_c=0.17$	$u_c=0.12$	$u_c=0.22$	$u_c=0.17$	$u_c=0.12$
5	2,798	2,678	2,818	2,658	2,568	2,668	2,928	2,788
5	2,808	2,688	2,828	2,668	2,578	2,678	2,938	2,798
7	2,486	2,416	2,476	2,386	2,326	2,366	2,586	2,496
7	2,496	2,426	2,486	2,396	2,336	2,376	2,596	2,506
10	2,232	2,202	2,202	2,162	2,142	2,122	2,312	2,272
10	2,242	2,212	2,212	2,172	2,152	2,132	2,322	2,282
15	2,02	2,02	1,98	2	1,97	1,92	2,08	2,07
15	2,03	2,03	1,99	2,01	1,98	1,93	2,09	2,08
20	1,91	1,92	1,85	1,86	1,89	1,81	1,95	1,96
20	1,92	1,93	1,86	1,87	1,9	1,82	1,96	1,97
30	1,787	1,817	1,717	1,747	1,777	1,687	1,817	1,837
30	1,797	1,827	1,727	1,757	1,787	1,697	1,827	1,847
40	1,711	1,751	1,651	1,691	1,721	1,621	1,741	1,771
40	1,721	1,761	1,661	1,701	1,731	1,631	1,751	1,781
50	1,667	1,707	1,607	1,647	1,687	1,577	1,697	1,727
50	1,677	1,717	1,617	1,657	1,697	1,587	1,707	1,737
60	1,641	1,681	1,571	1,621	1,661	1,551	1,661	1,701
60	1,651	1,691	1,581	1,631	1,671	1,561	1,671	1,711
80	1,591	1,641	1,521	1,581	1,621	1,511	1,611	1,651
80	1,601	1,651	1,531	1,591	1,631	1,521	1,621	1,661
100	1,562	1,612	1,502	1,552	1,602	1,482	1,582	1,632
100	1,572	1,622	1,512	1,562	1,612	1,492	1,592	1,642
120	1,544	1,594	1,474	1,534	1,584	1,464	1,564	1,604
120	1,554	1,604	1,484	1,544	1,594	1,474	1,574	1,614
160	1,515	1,575	1,455	1,505	1,565	1,435	1,535	1,585
160	1,525	1,585	1,465	1,515	1,575	1,445	1,545	1,595
200	1,505	1,555	1,435	1,495	1,545	1,425	1,515	1,565
200	1,515	1,565	1,445	1,505	1,555	1,435	1,525	1,575
240	1,485	1,545	1,425	1,485	1,535	1,415	1,495	1,545
240	1,495	1,555	1,435	1,495	1,545	1,425	1,505	1,555

*For each compartment, lower and upper limit are given for several values of the parameters
Each column correspond to a pair of parameters (pressure gradient and inner halftime)*

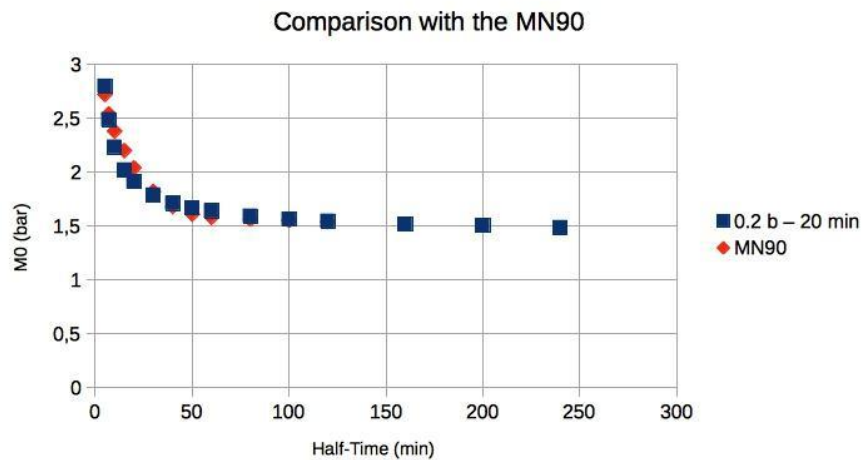


Fig. 9. Comparison of the best-predicted M-values with those used by the MN90 diving tables

Fig. 11 compares the evolution of the nitrogen tension, computed according to our theory or classical models, for a compartment of halftime 40 minutes initially saturated and brought back to the surface. Slightly larger quantities of nitrogen remain for a slightly longer time than predicted within the frame of classical models using exponential laws instead of Eq. 19 and Eq. 20. Fig.12 shows what happens, with air, when a compartment of halftime 40 minutes and that has spent 20 minutes at a pressure of 7.0 b (tantamount to diving at a depth of 60 m) is directly brought back to the surface. During this simulation, classical models would predict the occurrence of decompression accidents when the tension is higher than the $M0$ value, during the first 28 minutes after surfacing. Our theory predicts, more realistically, that decompression accidents cannot occur before an initial period, but can also happen more than one hour after surfacing. The few minutes after surfacing and before possible decompression problems are used by several tables to resume the decompression either underwater or in a decompression chamber. This kind of procedure cannot be explained within the frame of classical models: they compare only the current tensions of inert gases with static tabulated M-Values (Yellow horizontal line on Fig. 11). On the contrary, our theory links the delayed occurrence of symptoms with the gas phase extension. It explains why symptoms can occur later, at any moment when $u > u_c$. (Green curve on Fig. 11). It exists a correlation between the risk level and

the extension of the gas phase: $u=0$ corresponds to no risk and $u=u_c$ corresponds to a high risk. A quantitative link between u and the risk level may exist, although our theory is not capable to establish it yet. u may have more significance than the extension of a gas phase in a compartment.

Our theory justifies also very well the benefits of breathing pure oxygen. With the same scenario that Fig. 12, Fig. 13 shows what happens when oxygen is breathed after surfacing. The theory, as well as classical theories, predicts a faster decrease of the nitrogen tensions. However, Eq. 21 shows also that the predicted extension of the gas phase is reduced and that it remains for less time. This is a deeper and more quantitative explanation of the notion of “oxygen window.” The benefits of oxygen therapy without recompression are more apparent within the frame of this new theory. The main aim of the present article is not the engineering of precise decompression procedures. This is why we do not insist on many other common practices that can be justified with the same analysis based on “reducing the extension of the gas phase:” using pure oxygen at the 6m (20 feet) stop, using mixes with a higher proportion of oxygen than air (“nitrox”) during the decompression, etc. This is also why, in the present state, we do not present comparisons between decompression schedules issued from our theory and decompression schedules issued from tables or models, neo-Haldanian as well as RGBM and VPM.

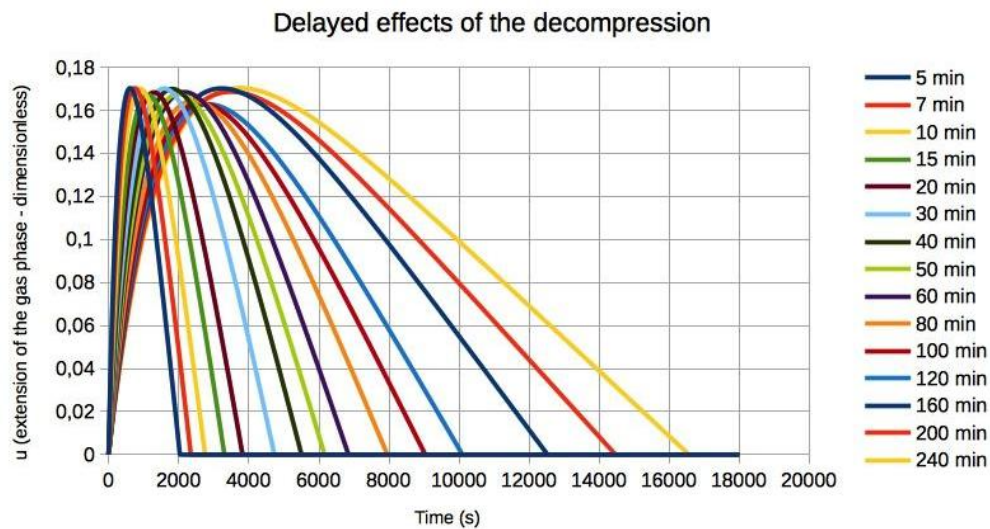


Fig. 10. Evolution of u (extension of the gas phase) during the desaturation
Each line corresponds to a different compartment or different halftime

Desaturation: comparison of the model with classical exponential laws

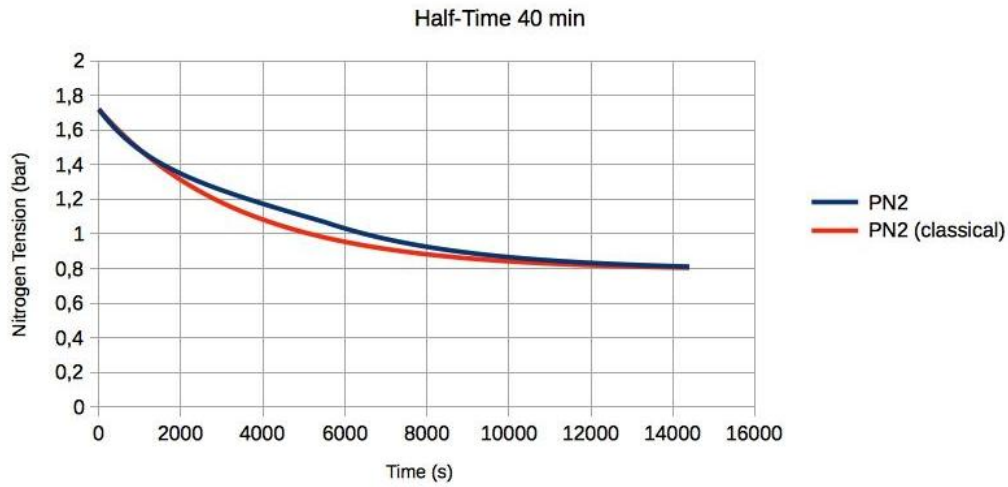


Fig. 11. Desaturation

Due to the gas phase, the desaturation is slower and no longer obeys exponential laws

Missing the stops - Comparison with classical theories

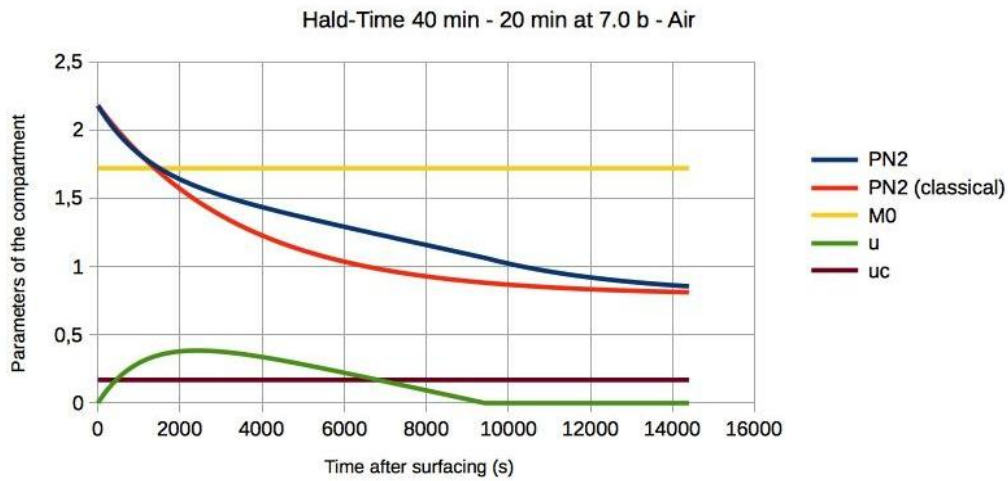


Fig. 12. Evolution of the gas phase and the tensions of inert gas in a single compartment when missing a stop

*The gas phase (green line) do not take its maximal extension immediately after surfacing
The unit for the tension or M-Values is the bar
u is dimensionless*

3.3 The Case of Helium or Mixes

3.3.1 Adequacy with workman M-values

Retaining $\delta P = 0.2$ bar and r' corresponding to a halftime of 20', with $u_c = 0.17$, Table 2 presents the predicted surface M-Values ($M0'$) of our theory for compartments that are saturated with

helium, then brought back to the surface and desaturated with air or with normoxic heliox. Fig. 14 shows the good adequacy between the values given by Workman and the values we calculated in the case of a compartment limited by perfusion (same halftimes for nitrogen and helium).

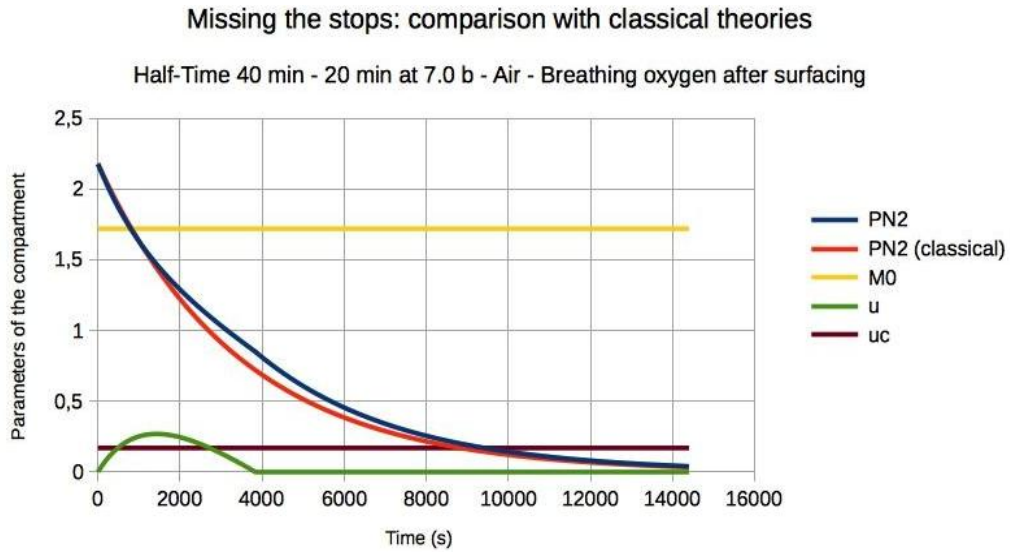


Fig. 13. Evolution of the gas phase and the tensions of inert gas in a single compartment when missing a stop and breathing pure oxygen after surfacing
The gas phase (green line) has a reduced extension
The unit for the tension or M-Values is the bar
u is dimensionless

3.3.2 Adequacy with Bühlmann M-Values

Bühlmann M-Values use halftimes that are different from several other models, including ours. However, Fig. 15 shows the rather good adequacy with the values predicted by our theory in the case of compartments limited by diffusion

(halftimes for helium lower than halftimes for nitrogen). The M-Values of the fastest compartments is considerably higher than their nitrogen counterpart. It is coherent with the fact that helium diffuses faster out of the compartments: less helium remains to sustain the formation of a gas phase (Eq. 22).

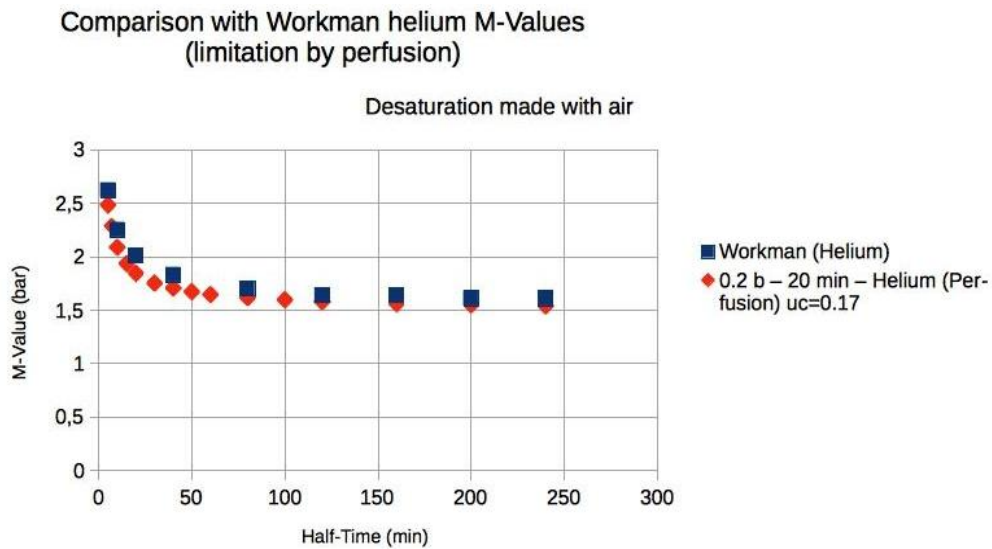


Fig. 14. Helium M-values predicted by the theory: Comparison with workman

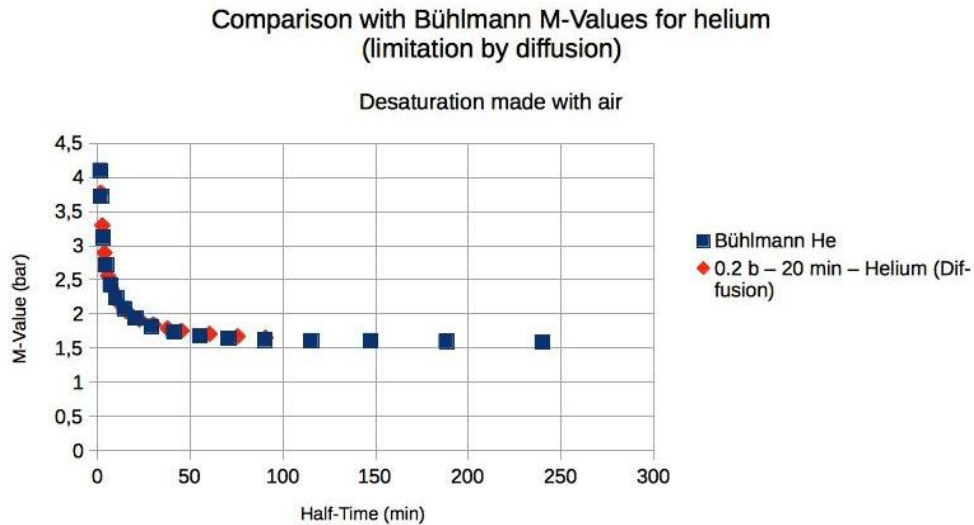


Fig. 15. Helium M-Values predicted by the theory: comparison with Bühlmann
For each compartment, a lower limit and an upper limit are given
Each column correspond to different cases
Gradient pressure 0.2 b and inner halftime 20 min

3.3.3 Shortcomings of the classical models

Table 3 presents, for the compartments having nitrogen half-times of 5 min and 240 min, the value of u_c when they are brought back to the surface and desaturated with air after having been saturated with trimix; the tensions corresponding to the criterion $P_{N_2} / MO + P_{He} / MO' = 1.0$

The fact the value of u_c is almost constant demonstrates that, when using mixes and combining M-Values, this criterion is more relevant than the criteria proposed by classical models (The one of Bühlmann) in [13] having been presented in 2.2). However, this remains a static criterion, whereas the decompression is a dynamical process: the tolerance of a compartment to inert gases does not depend only upon the tensions of nitrogen and helium inside, but also on the mix used for the desaturation, as already exemplified by Fig. 13. Only a dynamical model can correctly predict the tolerance to mixes of helium and nitrogen. The last column of Table 2 exemplifies the fact that, when brought back to the surface, compartments saturated with helium are less tolerant when the desaturation is carried out with normoxic heliox instead of air. In addition to that problem, many classical models assume that saturation and desaturation are either only limited by perfusion or only limited by diffusion. Intermediate

situations should be taken into account, as in Table 2.

3.4 General Discussion

3.4.1 Imperfections and limits of the theory

In its present state, our theory does not take in account the tensions of water and carbon dioxide (Eq. 3 and Eq. 4) inside the gas phase when it exists. Such a refinement would certainly modify the quantitative predictions. During the desaturation, circulating bubbles are trapped and eliminated when blood circulates through lung capillaries. If the blood itself is regarded as a compartment, this means that Eq. 13 and Eq. 14 are no longer verified in this case: the inert gases may be eliminated at a faster pace. In the case of very brutal decompressions, with a gas phase of large extension, Eq. 13 and Eq. 14 may also no longer be verified. Taking in account such phenomena would also certainly alter the quantitative predictions. Currently, we have not performed computations taking in account these two effects.

Taking into account more precisely the shape of the gas phase (Fig. 16) could lead to a pressure gradient depending upon its extension. Instead of being a constant parameter to tune, δP would become an unknown function to guess. It is tantamount to introducing more degrees of freedom in the theory and rendering it more empirical anew.

Table 2. Theoretical predictions of helium M-values

T (min) for N2	Perfusion – deco with air <i>uc=0.17</i>	Diffusion – deco with air <i>uc=0.17</i>	Intermediate – deco with air <i>uc=0.17</i>	Perfusion – deco with 21/79 heliox <i>uc=0.17</i>
5	2.475	3.77	3.025	2.355
5	2.485	3.78	3.035	2.365
7	2.255	3.29	2.705	2.165
7	2.265	3.3	2.715	2.175
10	2.082	2.89	2.435	2.01
10	2.092	2.9	2.445	2.02
15	1.93	2.555	2.208	1.88
15	1.94	2.565	2.218	1.89
20	1.84	2.37	2.072	1.8
20	1.85	2.38	2.082	1.81
30	1.747	2.16	1.935	1.727
30	1.757	2.17	1.945	1.737
40	1.701	2.045	1.854	1.681
40	1.711	2.055	1.864	1.691
50	1.667	1.96	1.799	1.647
50	1.677	1.97	1.809	1.657
60	1.641	1.915	1.762	1.631
60	1.651	1.925	1.772	1.641
80	1.611	1.84	1.718	1.601
80	1.621	1.85	1.728	1.611
100	1.592	1.785	1.681	1.582
100	1.602	1.795	1.691	1.592
120	1.574	1.75	1.655	1.574
120	1.584	1.76	1.665	1.584
160	1.555	1.705	1.628	1.555
160	1.565	1.715	1.638	1.565
200	1.545	1.67	1.6	1.545
200	1.555	1.68	1.61	1.555
240	1.535	1.65	1.59	1.535
240	1.545	1.66	1.6	1.545

For each compartment, a lower limit and an upper limit are given

Each column correspond to different cases

Gradient pressure 0.2 b and inner halftime 20 min

Table 3. Maximal extension of the gas phase with helium-nitrogen mixes

Halftime 5 min			Halftime 240 min		
Nitrogen tension (bar)	Helium tension (bar)	u_{max}	Nitrogen tension (bar)	Helium tension (bar)	u_{max}
2.8	0	0.170276	1.49	0	0.166881
2.52	0.248	0.169007	1.341	0.154	0.000154
2.24	0.496	0.167927	1.192	0.308	0.00017
1.96	0.744	0.167065	1.043	0.462	0.167357
1.68	0.992	0.166453	0.894	0.616	0.167454
1.4	1.24	0.166125	0.745	0.77	0.167532
1.12	1.488	0.166118	0.596	0.924	0.167598
0.84	1.736	0.16647	0.447	1.078	0.167664
0.56	1.984	0.167218	0.298	1.232	0.167745
0.28	2.232	0.168394	0.149	1.386	0.167863
0	2.48	0.170025	0	1.54	0.168052

For each compartment, a lower limit and an upper limit are given

Each column correspond to different cases, Gradient pressure 0.2 b and inner halftime 20 min

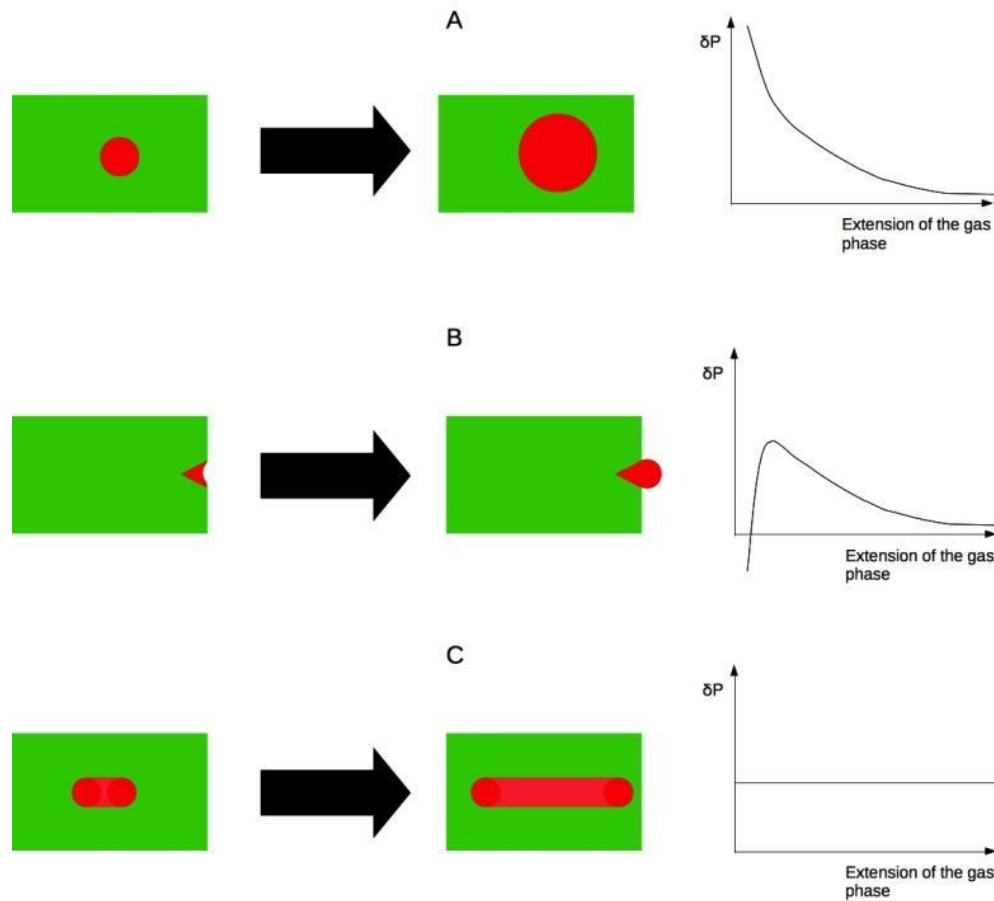


Fig. 16. Influence of the shape of the gas phase on the pressure gradient

Spherical bubbles (A), non-spherical bubbles (B) or a bubble developed in a blood vessel (C) have very different behaviours

3.4.2 Limits inherent to all the modelings

Because of obvious ethical reasons, the early experiments such as decompressing volunteers until they get symptoms of decompression sickness are impossible to reproduce. Models are improved on the basis of the statistics of incidents or accidents during the regular use of decompression procedures or tables [17,18]. On the one hand, the lower the frequency of an incident is, the less precise the determination of the corresponding probability is. On the other hand, not all the dive profiles are repeated a large number of times. Most of the recreational dives involve no or few decompression stops and the use of robots is preferred to very deep commercial dives. This relative lack of data regarding long and deep dives introduces a bias when validating or evolving decompression models. Another source of incertitude is the

personal variability and the lack of standardization of the few extreme dives performed by technical divers. Even if it fits the no-stops limit well, in its present state, the present theory is not developed into a full validated decompression model. However, other models regarded as fully validated might be, in fact, very deficient when used far from the no-stop limit [19,20].

3.4.3 Explanatory power

In its presents state, our theory gives rather good quantitative predictions. It fits the no-stop limits well and explains that the affine variations of the M-Value according to depth. However, its main interest remains the qualitative view it gives of the desaturation process. During a safe desaturation process, u remains lower than u_c . It first increases at the beginning of a decompression

stop, then decreases and vanishes if the stop is long enough. During unsafe dives, for example, missing the stops or using inadequate mixes, u will increase above u_c , in a delayed way. From that point of view, it is more complete than theories whose unique goal is "calculating the decompression stops."

In our theory, the smaller the extension of the gas phase inside a compartment is, the faster the gas disappears. This is an alternative explanation to the efficiency [21] or inefficiency [22] of "deep stops:" stops that are done before the M-Values of inert gases are reached.

3.4.4 Perspectives

The most complete validation (or invalidation) of this theory needs the analysis of the largest possible number of dives, preferably with complex profiles and far away from the no-stops limit. The analysis of the profiles will enable to reconstruct the evolution of u for each compartment and to find with a lesser statistical uncertainty the best values of δP and r' . The remaining dispersion of these values is linked to the relevance of the theory. It must be noticed that most of the existing diving data banks ([23] for instance) are not freely available. Fig. 17 shows how our theory in its present state can be used to assess already existing decompression profiles or to optimize them. The evolution of u (45 compartments from 5 min to 200 min limited by perfusion, diffusion and in-between) has been computed in the case of the dive of duration 30 min at a depth of 250 fsw (approximately 75 m) using a 16% oxygen, 33% helium, 51% nitrogen mix, that is described in [24]. Two decompression schedules named "ZHL safer" and "RGBM safer" in [24], both using trimix and oxygen, have been examined. A third profile has been added, that is a modification of "ZHL safer" by the author. Its stops between 100 ft and 30 ft use a 40% oxygen, 60% nitrogen mix. Certain durations have been modified (in min/ft) as 5/90; 5/80; 10/70; 10/60. The duration of the two last stops using pure oxygen have also been modified as 28/20;1/10. Fig. 17A shows the depth profiles and Fig. 17B shows the evolution of u . Through the value of this parameter, the theory affords a new way of assessing diving profiles, instead of considering only the depth of the first stops (or how deep they are below the ceiling imposed by the M-Values) and the duration of each stop.

This benchmark shows that "RGBM safer" is the best during the first stops, but that "ZHL safer" is the best for the last stops and after surfacing. The values of u of both profiles are, by far, above the thresholds proposed in Table 1. This is not the case of the third profile: it can be regarded as safer, with u always below 0.13. The "RGBM safer" profile adds deeper stops, but they are too short to remove enough inert gas of the gas phase: this is why, during shallow stops that are too short, u can reach an important value. This is not the case of the third profile, where the deeper stops have been extended. Along with the use of a correct mix, this enables a faster reduction of the gas phase. This is why the two last stops can be shortened. With pure oxygen, doing a stop at 10 ft is always less efficient than doing it at 20 ft. Our theory explains why very well: at 20 ft the pressure inside the gas phase is higher, so it will dissolve faster, then be removed faster.

The case of cave diving has been evoked above. Certain dives include more than two long and deep stays in less than 24 hours: they are clearly outside the field of neo-Haldanian models and outside of the field of any decompression table. Instead of using arbitrary safety margins concerning the M-Values or the duration of certain stops, our theory, through u , affords an alternative and rational way of increasing the safety level of this kind of dive. The stops can be optimized so that u is never higher than the threshold of Table 1. All the calculations can even be made with a lesser value of u_{max} (for example 0.13 instead of 0.17 in the example of Fig. 17). Because cave diving often takes place far from any recompression chamber, alone and with efforts to do just after the end of the dive, hardened decompression profiles are necessary. Ordinary decompression schedules regarded as safe enough for recreative or technical diving may be inadequate. Our theory is a possible resource to improve that. It can be remarked, in Fig. 17 that after surfacing no gas phase remains in the case of the improved profile we propose, whereas this is not the case for "RGBM safer" and "Bühlmann safer." Finally, at the fringe but from the point of view of global safety: the process of optimizing u forces the diver to a deeper reflexion than if (s)he uses only a non-free software (such as "V-Planner" or "DecoPlanner") that provides her/him directly with profiles (s)he is unable to compute. This is an educational advantage.

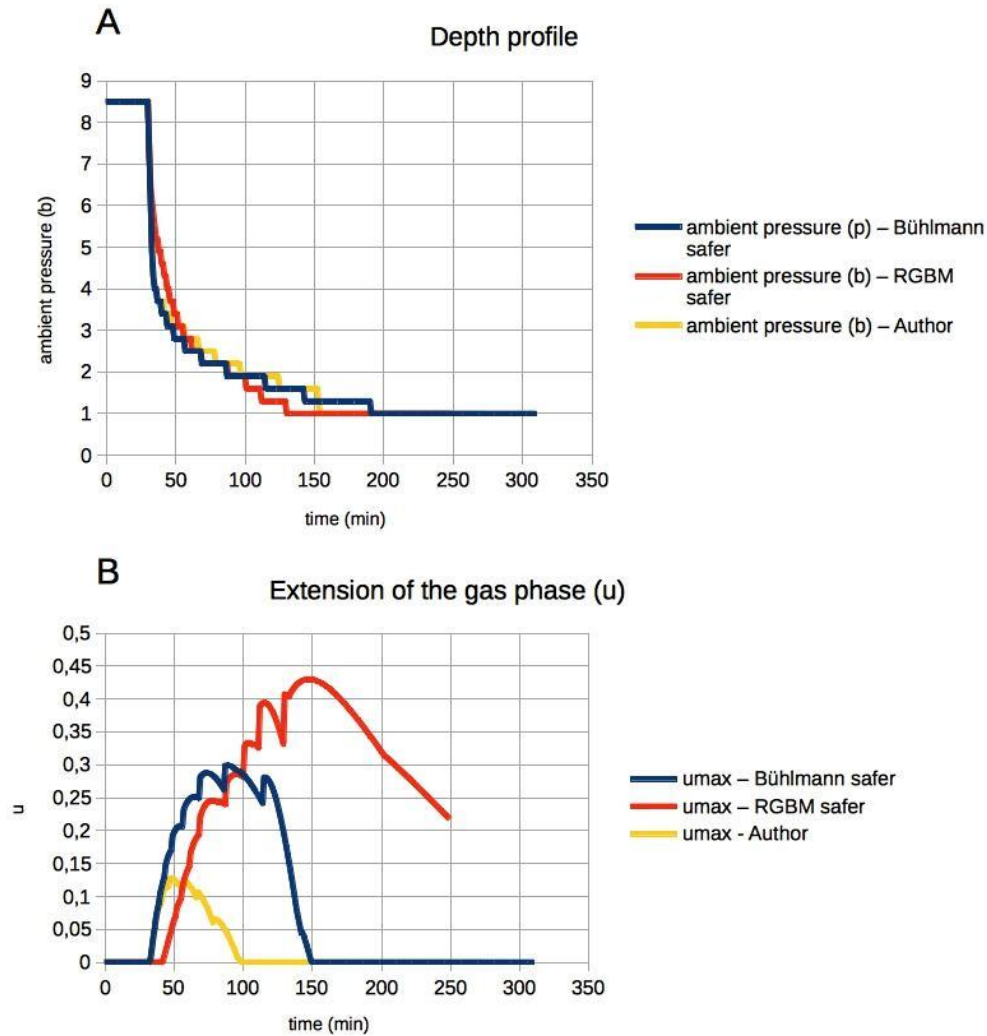


Fig. 17. Benchmark with a dive of duration 30 min at 250 ft using a 16% oxygen, 33%helium, 51% nitrogen, mix

A: depth profiles

B: evolution of u

Blue: Bühlmann. Red: RGBM. Yellow: optimisation by the author

4. CONCLUSION

This theory is simpler than RGBM and VPM. It is compatible with the static results of neo-Haldanian models (M-Values), but it has a larger explanatory power in the case of dynamical situations. Depending upon fewer parameters than RGBM and VPM, it is more parsimonious. With only three parameters, it can be tuned to give realistic values of MO and MO' for each compartment. It is capable, at least qualitatively, to explain the delayed occurrence of decompression problems. It is also capable of explaining the benefits of oxygen breathing

during normal or emergency procedures. It shows that the tolerance to inert gases depends on the composition of the mix that is breathed during the decompression. Clearly, the notion of M-Value is no longer relevant when using several mixes during a complex profile. Instead of delivering binary results such as “safe” or “unsafe”, the parameter u that represents the extension of the gas phase is linked to the risk level. Classical models that are regarded as perfectly validated may be deficient when applied to extreme dives, far from the no-stop limit. Even in its present state, our theory is a valuable tool in helping to assess such dive profiles. It goes far

beyond "calculating decompression stops:" already existing decompression schedules can be examined, and u computed during the different stops. Too large values during and after decompression indicate non-optimal profiles, possibly unsafe having in mind the statistical bias evoked in 3.4.2. Although it is not a systematically controlled study, it is worth to mention that, after some preliminary work [25], the author, as a cave diver, uses since 2010 his theory to assess the safety of each committed dive [26] he has to do.

ACKNOWLEDGEMENTS

I wish to thank the editors and the reviewers for the numerous exchanges we have had, in order to publish the best possible article.

COMPETING INTERESTS

Author has declared that no competing interests exist.

REFERENCES

1. Hempleman HV. History of decompression procedures. In: Bennett PB, Elliott DH, Editors. *The Physiology and Medicine of Diving*. 4th Revised Ed. Philadelphia: W B Saunders Co Ltd.; 1993.
2. Boycott AE, Damant GCC, Haldane JS. The prevention of compressed-air illness. *Epidemiology & Infection*. 1908;8(3):342-443.
3. Yount DE, Hoffman DC. On the use of a bubble formation model to calculate diving tables. *Aviation, Space, and Environmental Medicine*. 1986;57(2):149-156.
4. Wienke BR. Reduced gradient bubble model. *International Journal of Bio-medical Computing*. 1990;26(4):237-256.
5. Mitchell J, Doolette DJ. Extreme scuba diving medicine. In: Feletti F, Editor. *Extreme Sports Medicine*. 1st Ed. New York: Springer International Publishing; 2017.
6. Walsh C, Stride E, Cheema U, Ovenden N. A combined three-dimensional *in vitro-in silico* approach to modelling bubble dynamics in decompression sickness. *Journal of the Royal Society Interface*. 2017;14(137):20170653.
7. Howle LE, Weber PW, Hada EA, Vann RD, Denoble PJ. The probability and severity of decompression sickness. *PLoS One*. 2017;12(3):e0172665.
8. Angelini S. Dive computer decompression models and algorithms: Philosophical and practical views. *Underwater Technology*. 2018;35(2):51-61.
9. Workman RD. Calculation of decompression schedules for nitrogen-oxygen and helium-oxygen dives. Navy Experimental Diving Unit Panama City FL; 1965. (Accessed 23 July 2018) Available:<http://www.dtic.mil/dtic/tr/fulltext/u2/620879.pdf>
10. Bühlmann AA. Computation of low-risk compression. Computation model and results of experimental decompression research. *Schweizerische medizinische Wochenschrift*. 1988;118(6):185-197.
11. Blatteau JE, Guigues JM, Hugon M, et al. Plongée à l'air avec la table de décompression MN 90. Bilan de 12 années d'utilisation par la Marine française: à propos de 61 accidents de désaturation de 1990 à 2002. *Science & Sports*. 2005; 20(3):119-123. French with English Abstract
12. Imbert JP, Paris D, Hugon J, et al. The arterial bubble model for decompression table calculations. Proceedings of the 30th Annual Meeting of the European Underwater Baromedical Society. 2004;15-17. (Accessed 23 July 2018) Available:<http://gtuem.praesentiert-ihnen.de/tools/literaturdb/project2/pdf/Imbert%20JP.%20-%20EUBS%202004.pdf>
13. Baker EC. Understanding M-values. *Immersed-International Technical Diving Magazine*. 1998;3.
14. Sander R. Compilation of Henry's law constants (version 4.0) for water as solvent. *Atmospheric Chemistry & Physics*. 2015;15(8). (Accessed 11 August 2018) Available:<https://www.atmos-chem-phys.net/15/4399/2015/acp-15-4399-2015.pdf>
15. Piiper J, Worth H. Value and limits of Graham's law for prediction of diffusivities of gases in gas mixtures. *Respiration Physiology*. 1980;41(3):233-240.
16. D'Aoust BG, Smith KH, Swanson HT. Decompression-induced decrease in nitrogen elimination rate in Awake dogs. *Journal of Applied Physiology*. 1976;41(3): 348-355.
17. Howle LE, Weber W, Nichols JM. Bayesian approach to decompression sickness

- model parameter estimation. *Computers in Biology and Medicine*. 2017;82:3-11.
18. Cialoni D, Pieri M, Balestra C, Marroni A. Dive risk factors, gas bubble formation, and decompression illness in recreational SCUBA diving: Analysis of DAN Europe DSL data base. *Frontiers in Psychology*. 2017;8:1587. (Accessed 15 August 2018) Available:<https://www.frontiersin.org/articles/10.3389/fpsyg.2017.01587/full>
 19. Wienke BR, O'Leary TR, Del Cima OM. Empirical bubble broadening and effects on decompression schedules. *J Appl Biotechnol Bioeng*. 2018;5(3):193-200.
 20. Buzzacott P, Papadopoulou V, Baddeley A, Nadan MP, Folke L. Theoretical tissue compartment inert gas pressures during a deep dive with and without deep decompression stops: A case analysis. *International Maritime Health*. 2015;66(1): 36-42. (Accessed 15 August 2018) Available:<https://journals.viamedica.pl/international-maritime-health/article/view/41505>
 21. Baker EC. Clearing up the confusion about deep stops. *Immersed-International Technical Diving Magazine*. 1998;3.
 22. Guenzani S, Mereu D, Messersmith M, Arena M, Spanò A. Inner-ear decompression sickness in nine trimix recreational divers. *Diving Hyperb Med*. 2016;46(2):111-116. (Accessed 16 August 2018) Available:[http://www.eubs.org/documents/DHM%20Vol46\(2\).pdf#page=45](http://www.eubs.org/documents/DHM%20Vol46(2).pdf#page=45)
 23. Imbert JP, Bontoux M. Diving data bank: A unique tool for diving procedures development. *Offshore Technology Conference*; 1988. DOI: 10.4043/5707-MS (Accessed 14 September 2018) Available:<https://www.onepetro.org/conference-paper/OTC-5707-MS>
 24. Wienke BR, O'Leary TR. Deep RGBM. *Advanced Diver Magazine*. 2006;14. (Accessed 27 September 2018) Available:<http://www.advanceddivermagazine.com/articles/rgbmphase/rgbmphase.html>
 25. Boudinet P. Modélisation théorique de la croissance des bulles lors de la décompression et calcul théorique de M-Values (première partie). *Sifon* 1997;25: 25-31. French without EN Abstract (Accessed 19 October 2018) Available:<https://issuu.com/aquacorps/docs/sifon35>
 26. Boudinet P. Topographie de quelques siphons dans le Doubs. *Spelunca* 123. Gap: Gap Éditions; 2011. French without EN Abstract

© 2018 Boudinet; This is an Open Access article distributed under the terms of the Creative Commons Attribution License (<http://creativecommons.org/licenses/by/4.0>), which permits unrestricted use, distribution, and reproduction in any medium, provided the original work is properly cited.

Peer-review history:
The peer review history for this paper can be accessed here:
<http://www.sciencedomain.org/review-history/27021>